

A Highly Miniaturized Ultra-Wideband Antenna with a Triple-Band Notch for Wearable Applications

M. A. A. Rashid¹, S. M. Shah², H. A. Majid², A. Ponniran¹, and F. Hassan³

¹ Faculty of Electrical and Electronic Engineering, Universiti Tun Hussein Onn Malaysia, Johor, Malaysia

² Research Center for Applied Electromagnetics, Universiti Tun Hussein Onn Malaysia, Johor, Malaysia

³ School of Electrical Engineering, Faculty of Engineering, Universiti Teknologi Malaysia, Malaysia

Email: azzahramunirah@gmail.com; shaharil@uthm.edu.my; mhuda@uthm.edu.my; asmar@uthm.edu.my; fazilah.hassan@utm.my

Abstract—In this paper, a compact UWB antenna with a triple-band notch for wearable applications is designed and simulated for Ultra-Wideband (UWB) applications with the operating frequency from 3.1GHz to 10.6GHz. The antenna can be used for UWB applications, while at the same time, is able to reject the narrowbands namely, WiMAX (3.2GHz to 3.6GHz), C-band (3.7GHz to 4.2GHz) and WLAN (5.15 GHz to 5.35GHz). Two slots are introduced on the radiating patch of the antenna to notch the three narrowbands, instead of three slots to notch each narrowband. The antenna is designed on a semi-flexible Rogers Duroid RO3003™ substrate. The final outcomes indicate that the antenna can operate over the UWB frequency from 3.09 GHz to 11.09GHz. The antenna is able to notch the WiMAX and C-bands with a frequency range from 3.16GHz to 4.20 GHz and the WLAN band with a frequency range from 5.14 GHz to 5.34GHz. The performance of the antenna in bending condition is also examined with the antenna bent over a varying diameter of vacuum cylinder starting from 50mm, 80mm and 100mm. It is shown from the reflection coefficient of each diameter that the performance of the antenna is not affected by bending and thus, is particularly useful to be worn on body for wearable applications, other than its compact size of 19mm×14mm. The SAR results obtained shows that the antenna obeys the guidelines for 1mW of input power.

Index Terms—Bandwidth, bending investigation, electromagnetic, ultra-wideband, wearable antenna, wireless local area network, worldwide interoperability for microwave access

I. INTRODUCTION

The growth of wireless communications nowadays has increased the demand for a mobile device to support multiple applications but yet still maintaining a small and compact size of the antenna. A miniaturized wearable electronic device with an Ultra-Wideband (UWB) technology is able to serve the requirements of an extremely high data transmission rate with a limited

range, connect all devices that a person carries and interact with one another. Restrictions on the transmitted power by the FCC to simultaneously allow other communications in 3.1GHz to 10.6GHz band make UWB a technology of choice for wireless indoor and wearable applications such as room automation and Wireless Body Area Network (WBAN) [1]-[4].

According to IEEE 802.11a, for an UWB antenna to work in wearable and indoor applications, it should avoid the higher band with a frequency range from 5.15GHz to 5.35GHz, assigned for Wireless Local Area Network (WLAN) [5]. Meanwhile, a few other signal spectrums such as, C-band (3.2GHz to 3.6GHz) and WiMAX (3.7 GHz to 4.2GHz) can also cause interference with their neighboring channels [6]-[8]. Therefore, the overall performance of UWB systems can be very much degraded in terms of bit error rate and also creating pulse distortions [9]. For that reason, it has become an obligation to design UWB antennas with band notched characteristics to ensure a robust and interference-free UWB antenna.

Specific Absorption Rate (SAR) is described as a degree of rate at which energy is absorbed by the body when exposed to an electromagnetic field from an antenna [10]. The SAR limit set by the FCC is 1.6W/kg averaged over 1g of actual tissue while the SAR limit recommended by the International Commission on Non-Ionising Radiation Protection (ICNIRP) is 2.0W/kg averaged over 10g of actual tissue [11]. Influence of body proximity on the performance of antenna and the amount of SAR absorbed by human body are the two significant on-body measurements for wearable antennas.

Introducing parasitic strips near the radiation patch or ground plane has been attempted to notch the unwanted narrowbands [12]-[13]. Other methods have also been used such as by embedding a pair of T-shaped stubs inside an elliptical slot in the radiation patch, inserting a complementary split-ring resonator near the feed line, or by using a coupled C-shaped parasitic structure [14]-[19]. Each notch structure can only rejected one unwanted band. Therefore, to yield multiple notched bands, multiple notch structures are necessary. This in return,

Manuscript received May 28, 2021; revised August 15, 2021; accepted September 21, 2021.

Corresponding author: S. M. Shah (Email: shaharil@uthm.edu.my)

The research was carried out under the Internal University Grant of Tier 1 (Code No: H154) provided by Universiti Tun Hussein Onn Malaysia.

will introduce complexity to the antenna’s design and configuration.

In this work, an UWB antenna is proposed which can be particularly useful for wearable applications. In order to alleviate a potential electromagnetic interference arises from the narrowband applications namely, WiMAX (3.2GHz to 3.6GHz), C-band (3.7GHz to 4.2GHz) and WLAN (5.15GHz to 5.35GHz), notch bands are intro-

duced to discard the unwanted narrow-bands [20]-[25]. Table I compares the size and characteristics of proposed antenna with previous work on wearable UWB antenna with notch bands. The highly compact size of the antenna not only caters to the need of a compact size antenna to support multiple applications but is also particularly useful for wearable applications if the antenna is to be worn on body.

TABLE I: COMPARISON OF THE PROPOSED ANTENNA WITH PREVIOUS WORK ON WEARABLE UWB ANTENNA WITH NOTCH BANDS

Reference	Size of antenna (mm ²)	Impedance Bandwidth	Notch bands	Frequency of Notch Bands	Substrate
[2]	12×19	2.95 GHz to 12 GHz	WiMAX WLAN X-band	3.3 GHz – 3.8 GHz 5.15 GHz – 5.825 GHz 7.25 GHz – 7.75 GHz	FR-4
[17]	26×16	3.1 GHz to 10.6 GHz	WLAN	5.25 GHz	Ultra-thin liquid crystal polymer (LCP)
[18]	49×34	3.1 GHz to 10.6 GHz	WLAN	5 GHz	PET film
[24]	27×21	3.1 GHz to 10.6 GHz	C-band WLAN	3.7 GHz – 4.2 GHz 5.15 GHz – 5.825 GHz	Ultra-thin liquid crystal polymer (LCP)
[25]	16×25	3 GHz to 10.7 GHz	WLAN WiMAX	5.15 – 5.825 GHz 5.25 GHz – 5.85 GHz	FR-4
Proposed Antenna	19×14	3.09 GHz to 11.09 GHz	WiMAX C-band WLAN	3.2 GHz – 3.6 GHz 3.7 GHz – 4.2 GHz 5.15 GHz – 5.35 GHz	Rogers Duroid (RO3003™) Semi-Flexible Substrate

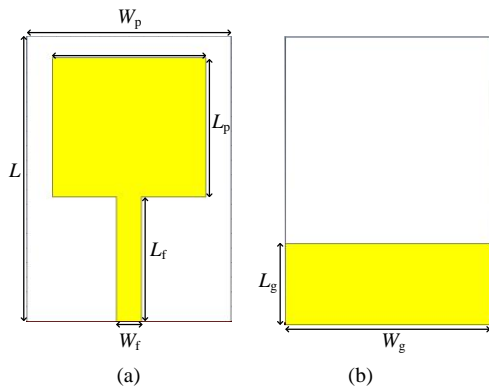


Fig. 1. Fundamental UWB antenna: (a) Top view and (b) Bottom view

TABLE II: DIMENSIONS OF THE FUNDAMENTAL UWB ANTENNA

Parameter	Values (mm)
L	19
W	14
L_p	14.5
W_p	10.5
L_f	8.5
W_f	1.5
L_g	5.5
W_g	14

II. RESEARCH METHODOLOGY

This section explains the method used in order to obtain the results of the work, including the design stage and the simulation stage that are performed by using CST MWS® software.

A. Fundamental UWB Antenna Design and Configuration

The fundamental UWB antenna is the outcome from optimization process based on the basic microstrip patch antenna. A standard rectangular patch antenna with a microstrip feed line to connect the waveguide port to the radiating patch and a full ground plane is designed at the

preliminary stage. A partial ground plane approach is then applied to increase the frequency range and operate from 3.1GHz to 10.6GHz for UWB. The proposed UWB antenna can be seen in Fig. 1 and the dimensions of the antenna are listed in Table II.

B. Design and Configuration of the UWB Antenna with Notch Bands

In order to achieve an UWB antenna with band notch characteristics, a first slot is introduced on the radiating patch to simultaneously reject the WiMAX and C-bands. The second slot is introduced to notch the WLAN band. At the final stage, both slots are combined into a single UWB antenna to reject the three narrowband applications.

1) UWB antenna with a slot to notch the WiMAX and C-bands

Commonly, one slot is used to notch one frequency band. However, in this work, one slot is used to notch two narrowbands as WiMAX and C-bands are a close neighboring application with WiMAX band from 3.2 GHz to 3.6GHz and C-band from 3.7GHz to 4.2GHz. In addition, by using only one slot to notch the two narrowbands, complexity of the antenna is reduced which in return will ease the fabrication process. A rigorous parametric study has been performed to obtain the best location and dimensions of the inverted-L slot on the radiating patch. Fig. 2 (a) shows the UWB antenna with an inverted-L slot to notch the WiMAX and C-narrowbands.

2) UWB antenna with a slot to notch the WLAN band

Similarly, another slot is engraved on the radiating patch of the antenna to notch the WLAN narrow bands from 5.15GHz to 5.35GHz (lower band WLAN) [24], [26] as shown in Fig. 2 (b). Parametric study has been conducted to obtain the best position and dimensions of the slot (from a combination of one U-slot and two inverted-U slots) to reject the WLAN narrow band. The geometry and dimensions of the radiating patch and

ground plane are similar to the previous antenna to notch the WiMAX and C-band narrow bands.

3) *UWB antenna with a triple band notch (combination of both slots bands)*

In the final antenna design, which is the main goal of this work, two slots from the previous UWB antennas are combined to notch all the three narrowbands intended for WiMAX, C- and WLAN applications. The dimensions of the slots have been optimized to obtain the best narrowbands without increasing the overall size of the antenna. Fig. 2 (c) shows the final design of the UWB antenna with a triple-band notch characteristic. Table III lists the dimensions of the two slots on the radiating patch.

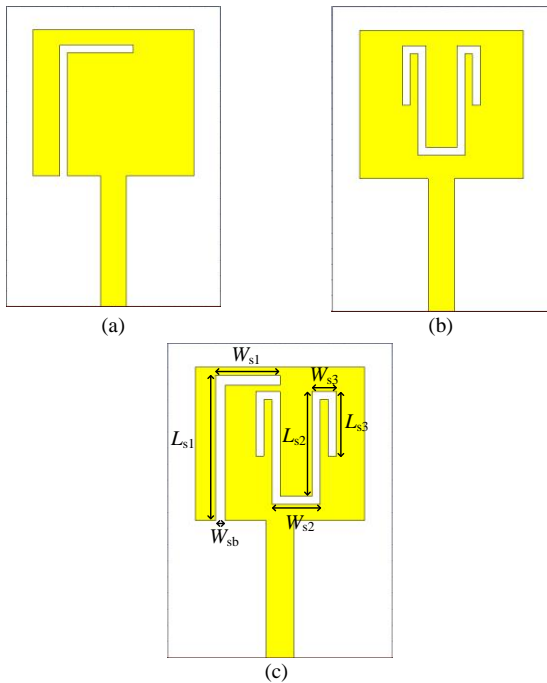


Fig. 2. UWB antenna to reject the: (a) WiMAX and C- bands, (b) WLAN band, and (c) WiMAX, C- and WLAN bands

TABLE III: DIMENSIONS OF THE FUNDAMENTAL UWB ANTENNA WITH A TRIPLE-BAND NOTCH

Parameter	Values (mm)
L_{s1}	9
W_{s1}	3.5
L_{s2}	7
W_{s2}	3
L_{s3}	3.5
W_{s3}	1.5
W_{sb}	0.5

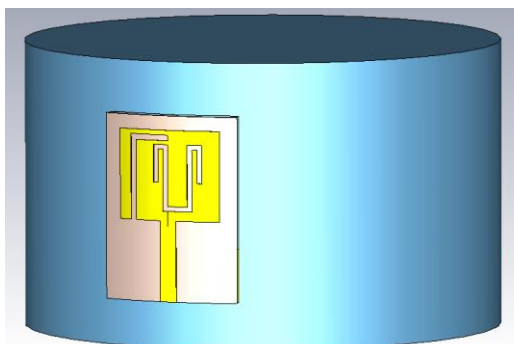


Fig. 3. Antenna curvature bending along the y-axis.

C. *Antenna Simulation in Bending Condition*

In order to perform bending investigation, a vacuum cylinder along y-axis is created to imitate the human arms as shown in Fig. 3. CST MWS[®] software is used to simulate the bending of antenna over the vacuum cylinder with varying diameters of 50mm, 80mm and 100mm. The sizes are selected based on the average approximate size of human arms.

III. RESULTS AND ANALYSIS

In this section, the simulated linear characteristics of the antennas on RO3003[™] are presented to investigate the performance in terms of reflection coefficient, maximum surface current distributions and bending condition. Furthermore, the SAR limit is simulated to satisfy the requirements enforced by the FCC and ICNIRP.

A. *Reflection Coefficient*

1) *Fundamental UWB antenna*

In Fig. 4, the UWB antenna operates within the frequency range of 3.09GHz to 11.09GHz, which fulfills the requirement of this work as the UWB frequency range governed by the FCC is from 3.1GHz to 10.6GHz. The bandwidth of the frequency range is 7.94GHz, which is wider than the standard frequency range. The reflection coefficient of this UWB antenna design is greater than 10 dB-line, implying that the antenna works well within the entire frequency range.

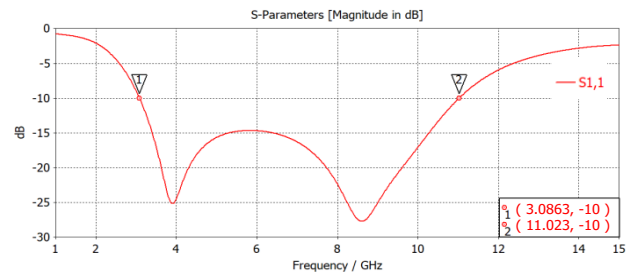


Fig. 4. Simulated reflection coefficient and bandwidth of the UWB antenna.

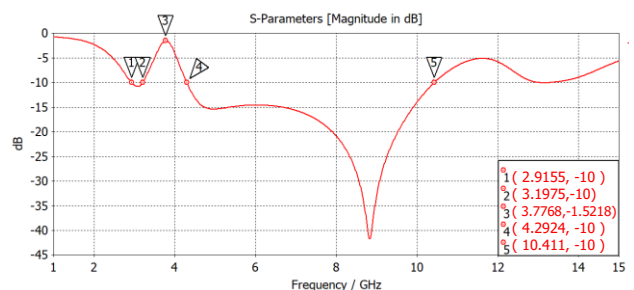


Fig. 5. Simulated reflection coefficient of the UWB antenna with a slot to notch WiMAX and C-bands.

2) *UWB antenna with a slot to notch the WiMAX and C-bands*

Fig. 5 shows the simulated reflection coefficient, S_{11} of the UWB antenna with the L-inverted slot on the radiating patch. From the figure, the antenna exhibits a good UWB bandpass performance from 2.92GHz to 10.41GHz with an impedance bandwidth of 7.49GHz. A desired band notch has been achieved which covers the

range of 3.20GHz to 4.30GHz with a midband frequency of 3.78GHz and bandwidth of 1.1GHz. This shows that the antenna can effectively avoid interference with the existing WiMAX (3.2GHz to 3.7GHz) and C-band (3.7GHz to 4.2GHz) systems.

3) *UWB antenna with a slot to notch the WLAN band*

Fig. 6 shows the simulated reflection coefficient, S_{11} of the UWB antenna with a second slot (combination of one U-slot and two inverted-U slots). From the figure, the antenna has a return loss less than 10dB-line at frequency range from 3.07GHz to 11.01GHz with notch bands between 5.11GHz and 5.38GHz. This implies that the antenna exhibits satisfactory performance at the entire UWB frequency range, while filtering out the middle and upper range of the WLAN band as stipulated by the Malaysian Communications and Multimedia Commission (MCMC) [27], as per required in this work. The desired notch frequency has the lowest reflection coefficient at 3.78GHz and covering approximately 270MHz bandwidth.

4) *UWB antenna with a triple-band notch (combination of both slots)*

Fig. 7 shows the simulated reflection coefficient of the UWB antenna with a combined WiMAX, C- and WLAN bands rejection. From the figure, the antenna operates within three frequency bands. The first band is from the frequency range of 2.89GHz to 3.16GHz with a bandwidth of 270MHz, the second band is from 4.20GHz to 5.14GHz with a bandwidth of 4.8696 GHz while the third band is from 5.34GHz to 10.56GHz with a bandwidth of 940MHz. Three notch bands are produced from the slots' combination. The WiMAX and C- notch band are within the frequency range from 3.16GHz to 4.20GHz while the WLAN notch band is within the frequency range from 5.14GHz to 5.34GHz. Therefore, the combination of both slots has successfully generated the required notch bands after some optimization of the dimensions of the antenna. The reflection coefficient plot exhibits strong rejection in the WiMAX and C-bands from 3.16GHz to 4.20GHz and WLAN band from 5.14GHz to 5.34GHz with a passband from 2.95GHz to 12GHz.

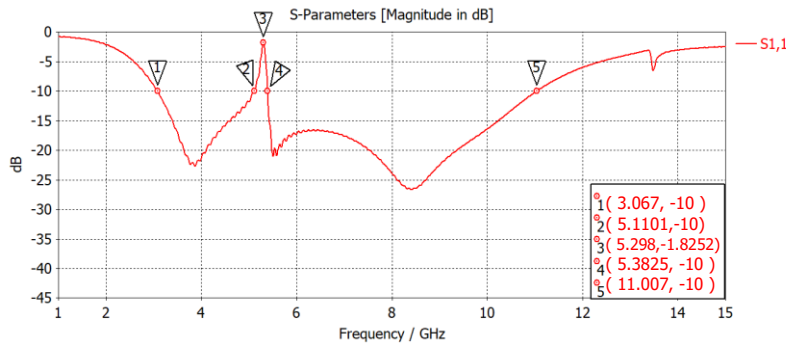


Fig. 6. Simulated reflection coefficient of the UWB antenna with a slot to notch WLAN band

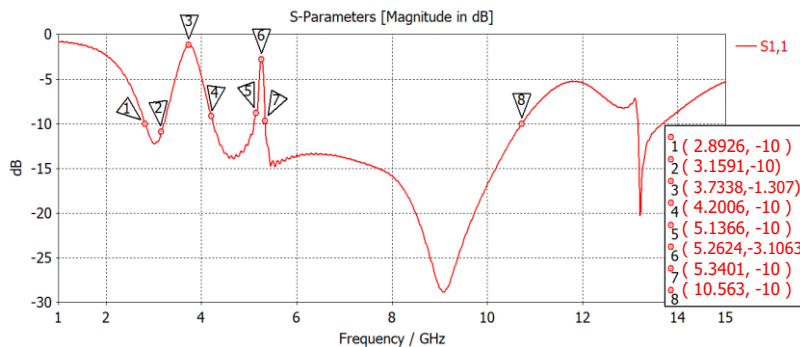


Fig. 7. Simulated reflection coefficient and bandwidth of the UWB antenna with a slot and copper strip to notch the WiMAX, C- and WLAN bands

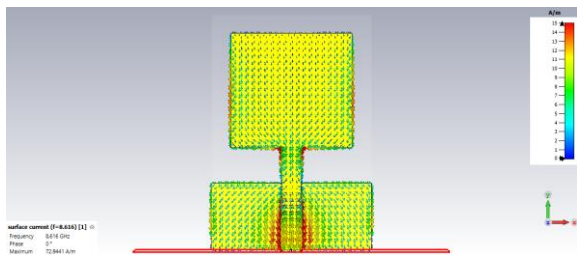


Fig. 8. Surface current distribution of the fundamental UWB antenna at 6.85 GHz.

B. *Surface Current Distribution*

Fig. 8 shows the surface current distribution of the UWB antenna at 6.85GHz. The frequency of 6.85GHz is

chosen as it is the location of the greatest reflection coefficient within the simulated frequency range. From the figure, maximum surface current is seen to be concentrated in the middle of the partial ground plane, which enhances the performance at middle operating frequency. Besides, a small area of maximum current can also be seen at the bottom edge of the radiating patch. This shows that the middle section of the ground plane and a small part of radiating patch are responsible in radiating electromagnetic waves from the antenna.

Fig. 9 illustrates current distribution of the UWB antenna with two slots to notch the WiMAX, C- and WLAN bands. Fig. 9 (a) shows that at 3.73GHz (the point of highest reflection coefficient of WiMAX and C-

bands), the maximum current distribution is concentrated around the first slot (inverted L-slot). The current distribution on the radiating patch is non-uniform and multi directional, implying the current distribution is disturbed hence results in notch bands for WiMAX and C- bands [28]. Besides, the maximum surface current is also seen in the upper and lower of the feedline and in the middle of partial ground plane of the antenna, indicating these parts are also responsible in blocking the electromagnetic waves from the antenna. Meanwhile, Fig. 9 (b) shows the surface current distribution of the UWB antenna at 5.26GHz, which is the point of highest reflection coefficient of WLAN notch bands. An apparent maximum current is seen to be concentrated around the second slot (combination of one U-slot and two inverted-U slots), indicating a large portion of electromagnetic energy has been stored around the slot rather than being radiated into the free space, so that the radiation efficiency decreases at the WLAN band [29]-[30].

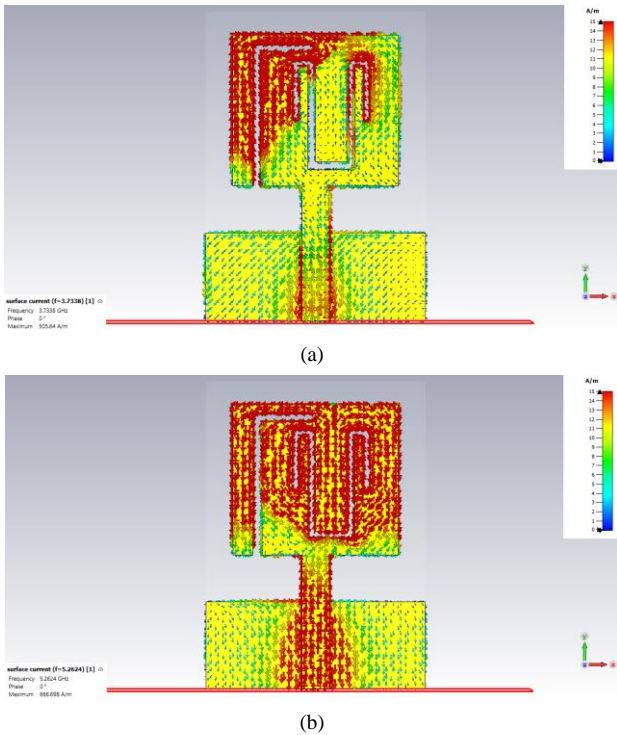


Fig. 9. Simulated surface current distribution of the UWB antenna with a slot and copper strip to notch the WiMAX, C- and WLAN bands at: (a) 3.73GHz and (b) 5.26GHz

C. Radiation Pattern

This antenna shows stable radiation patterns throughout UWB range as demonstrated in Fig. 10. At radiating frequencies of 3.1GHz and 6.85 GHz in Fig. 10 (a) and Fig. 10 (b), the antenna exhibits bidirectional patterns in the E-plane and omnidirectional patterns in the H-plane, indicating the antenna works well in the lower and middle UWB frequencies. Due to increasing harmonics of higher order modes, the radiation pattern in the E-plane is slightly distorted at a higher frequency of 10.6 GHz as shown in Fig. 10 (c). However, the antenna maintains an omnidirectional pattern in the H-plane.

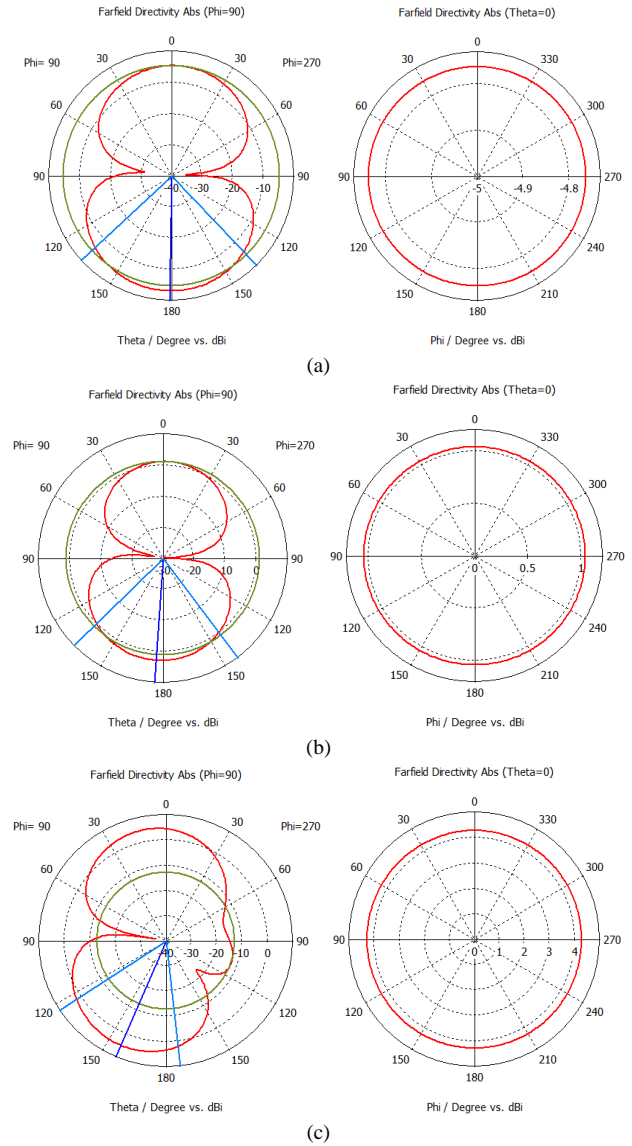
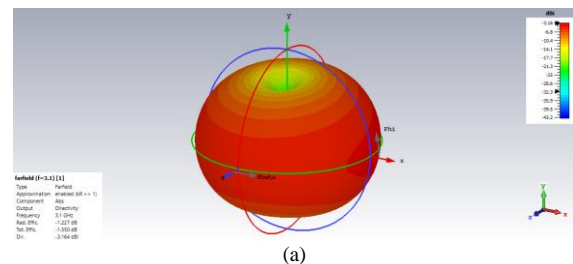


Fig. 10. Radiation patterns of the UWB antenna with a combined WiMAX, C- and WLAN bands rejection in the E-plane and H-plane at: (a) 3.1 GHz, (b) 6.85 GHz, and (c) 10.6 GHz.

D. Gain and Efficiency

Fig. 11 shows the gain and efficiency of the UWB antenna at 3.1GHz, 6.85GHz and 10.6GHz. The gain, G of the antenna at 3.1GHz is -3.164dBi and the efficiency, $\eta(\%)$ is 75.38%. The gain, G of the antenna at 6.85GHz is 2.780dBi and the efficiency, $\eta(\%)$ is 75.02%. At 10.6GHz, the gain, G is 4.989dBi and the efficiency of the antenna, $\eta(\%)$ is 74.11%. The high gain at all frequencies except at 3.1GHz implies that the antenna operates well within the UWB frequency range.



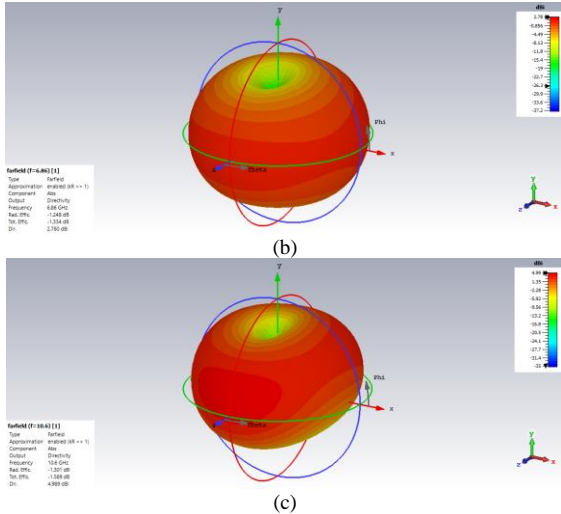


Fig. 11. Gain and efficiency of the UWB antenna with a combined WiMAX, C- and WLAN bands rejection at: (a) 3.1 GHz, (b) 6.85 GHz, and (c) 10.6 GHz.

E. Bending Investigation

The simulated reflection coefficient of the antennas in three bending conditions can be viewed in Fig. 12. From the figure, the reflection coefficients are similar when the antenna is bent over a vacuum cylinder with 80 mm and 100 mm in diameters. A slight difference is observed for the vacuum cylinder with 50 mm in diameter at the upper frequency range from 9 GHz to 12GHz. It is observed that the return loss is almost keep unchanged when different diameter of cylinder is applied. It is because besides having a small size of antenna, the designed slots are placed only on the radiating patch, thus minor changes of input impedance and resonant frequency are brought when the antenna is bent. It is evident from these results that the antenna maintains satisfactory performance for the whole UWB frequency range, while keeping the notch at the required narrow-bands under bending circumstances.

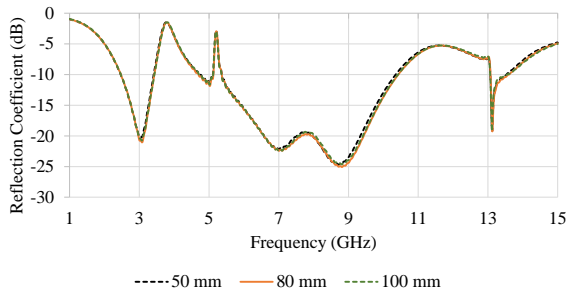


Fig. 12. Simulated reflection coefficients of the UWB antenna with a triple-band notch in bending condition over a vacuum cylinder with varying diameters of: (a) 50mm, (b) 80mm, and (c) 100mm.

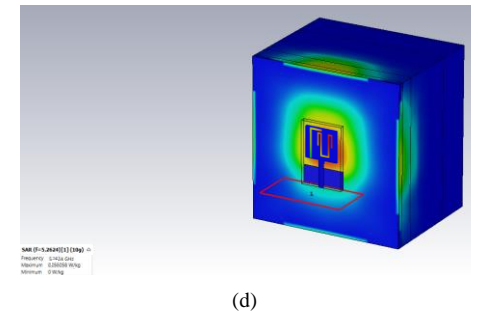
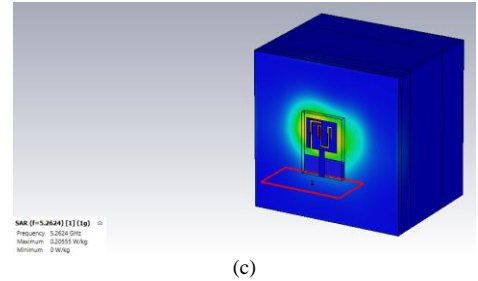
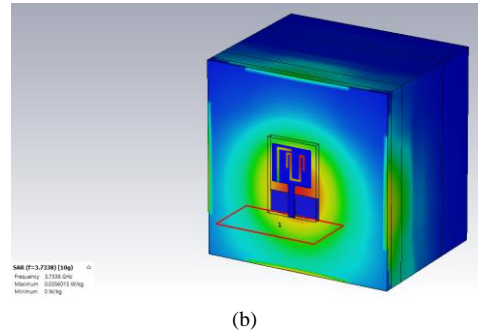
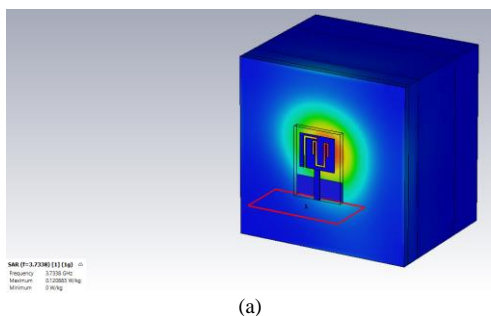


Fig. 13. Simulated SAR values of the UWB antenna with a triple-band notch at: (a) 3.73 GHz for 1g of human tissue, (b) 3.73 GHz for 10g of human tissue, (c) 5.26 GHz for 1g of human tissue, and (d) 5.26 GHz for 10g of human tissue

F. Specific Absorption Rate

Every antenna intended for wearable application needs to obey the SAR level that have been stipulated by the FCC and ICNIRP, which are the SAR should not be greater than 2W/kg averaged over 10g and not greater than 1.6W/kg averaged over 1g of the human tissue. The input power for the antenna to calculate the SAR is selected at 1mW, as commonly practiced. The antenna is located at 2mm above phantom tissue layers to cater for the thickness of a fabric if the antenna is to be worn on body. The calculation of SAR level is based on the IEEE C95.1 standard provided in the CST MWS software. Fig. 13 shows the result of the SAR simulation of the UWB antenna with triple notch bands at 3.73GHz and 5.26GHz. As can be seen in Fig. 13 (a), the SAR limits at 3.73GHz at 1mW input power to the antenna is 0.12W/kg for 1g of human tissue while for 10g is 0.04W/kg as in Fig. 13 (b). Thus, it shows that at 1mW input power, the SAR limits obey the guidelines by the FCC and ICNIRP and thus, the antenna is safe for on-body applications. Meanwhile, Fig. 13 (c) shows the SAR limits at 5.26GHz at 1mW input power to the antenna is 0.25W/kg for 1g of human tissue and 0.06W/kg for 10g as in Fig. 13 (d). Therefore, it indicates that the SAR limits obey the regulations by the FCC and ICNIRP at 1mW input power.

IV. CONCLUSION

In conclusion, a compact UWB antenna with a triple band notch function is presented in this work. Two slots on the radiating patch are introduced to achieve notch bands at WiMAX, C- and WLAN bands. The simulation results demonstrate that the UWB antenna can operate over the UWB frequency band from 3.09GHz to 11.09GHz (Actual UWB band: 3.1GHz to 10.6GHz) with the WiMAX and C-notch bands from 3.16GHz to 4.20GHz (Actual WiMAX band: 3.2GHz to 3.6GHz; Actual C-band: 3.7GHz to 4.2GHz) and WLAN notch band from 5.14GHz to 5.34GHz (Actual WLAN band: 5.15GHz to 5.35GHz). Simulation results in bending condition shows that performance of the UWB antenna is not affected when it is bent over a vacuum cylinder with varying diameters of 50mm, 80mm and 100mm, which represents different sizes of human arm. Therefore, the antenna is particularly useful in wearable applications given the unaffected performance in bending condition and its compact size of 19mm×14mm, which will avoid discomfort to the user when worn on body. SAR level investigation are also done to both antennas to ensure that they follow the requirement as guided by the FCC and ICNIRP. The SAR results obtained shows that the UWB antenna with a triple-band notch obeys the guidelines for 1mW input power. At 3.73GHz, the simulated SAR limits for 1g of human tissue is computed at 0.12W/kg (FCC standard: 1.6W/kg) while for 10g is at 0.04W/kg (ICNIRP standard: 2W/kg). At 5.26GHz, the SAR limits for 1g of human tissue is computed at 0.25W/kg while for 10g is at 0.06W/kg.

CONFLICT OF INTEREST

The authors declare no conflict of interest.

AUTHOR CONTRIBUTIONS

Munirah Az Zahra Abdul Rashid designed and simulated the antennas and also wrote the paper. Shaharil Mohd Shah analyzed the results and proofread the paper. Huda A Majid and Asmarashid Ponniran advised the results analysis and structure of the paper. All authors had approved the final version of the paper.

ACKNOWLEDGMENT

The author would like to acknowledge Universiti Tun Hussein Onn Malaysia for the financial assistance under the Internal University Grant of Tier 1 (Code No: H154).

REFERENCES

- [1] D. Yang, J. Hu, and S. Liu, "A low profile UWB antenna for WBAN applications," *IEEE Access*, vol. 6, pp. 25214–25219, Apr. 2018.
- [2] S. Doddipalli and A. Kothari, "Compact UWB antenna with integrated triple notch bands for WBAN applications," *IEEE Access*, vol. 7, pp. 183–190, Dec. 2018.
- [3] S. Yan, P. J. Soh, and G. A. E. Vandenbosch, "Wearable ultrawideband technology—A review of ultrawideband antennas, propagation channels, and applications in wireless body area networks," *IEEE Access*, vol. 6, pp. 42177–42185, July 2018.
- [4] J. Ali, N. Abdullah, R. Yahya, A. Joret, and E. Mohd, "Ultra-wideband antenna with monostatic/bistatic configurations for detection applications," *Int. J. Adv. Trends Comput. Sci. Eng.*, vol. 8, pp. 219–223, Aug. 2019.
- [5] Q. H. Abbasi, M. U. Rehman, X. Yang *et al.*, "Ultrawideband band-notched flexible antenna for wearable applications," *IEEE Antennas Wirel. Propag. Lett.*, vol. 12, pp. 1606–1609, Dec. 2013.
- [6] H. Hosseini, H. R. Hassani, and M. H. Amini, "Miniaturised multiple notched omnidirectional UWB monopole antenna," *Electron. Lett.*, vol. 54, no. 8, pp. 472–474, 2018.
- [7] M. S. Alam and A. Abbosh, "Reconfigurable band-rejection antenna for ultra-wideband applications," *IET Microwaves, Antennas Propag.*, vol. 12, no. 2, pp. 195–202, 2018.
- [8] S. Saxena, B. K. Kanaujia, S. Dwari, S. Kumar, and R. Tiwari, "A compact dual-polarized MIMO antenna with distinct diversity performance for UWB applications," *IEEE Antennas Wirel. Propag. Lett.*, vol. 16, pp. 3096–3099, Oct. 2017.
- [9] Y. Jalil, C. Chakrabarty, and B. Kasi, "A compact wideband microstrip antenna integrated with band-notched design," *European Journal of Scientific Research*, vol. 77, no. 4, pp. 477–484, 2012.
- [10] J. Trajkovikj and A. K. Skrivervik, "Comparison of SAR of UHF wearable antennas," in *Proc. 10th European Conf. on Antennas and Propagation (EuCAP)*, 2016.
- [11] International Commission on Non-Ionizing Radiation Protection. "Guidelines for Limiting Exposure to Time-Varying Electric, Magnetic and Electromagnetic Fields (up to 300 GHz)," *Health Physics*, vol. 74, no. 4, pp. 492–522, 1998.
- [12] F. Xu, X. Chen, and X. A. Wang, "UWB antenna with triple notched bands based on folded multiple-mode resonators," *IEICE Electronics Express*, vol. 9, no. 11, pp. 965–970, 2012.
- [13] D. Sarkar, K. V. Srivastava, and K. Saurav, "A compact microstrip-fed triple band-notched UWB monopole antenna," *IEEE Antennas Wirel. Propag. Lett.*, vol. 13, pp. 396–399, Feb. 2014.
- [14] M. A. R. Osman, M. K. A. Rahim, N. A. Samsuri, M. K. Elbasheer, and M. E. Ali, "Textile UWB antenna bending and wet performances," *Int. J. Antennas Propag.*, vol. 2012, 2012.
- [15] A. Salam, A. Khan, and M. Hussain, "Dual band microstrip antenna for wearable applications," *Microw. Opt. Technol. Lett.*, vol. 56, pp. 916–918, Apr. 2014.
- [16] M. Osman, M. K. A. Rahim, N. A. Samsuri, H. Salim, and M. Ali, "Embroidered fully textile wearable antenna for medical monitoring applications," *Prog. Electromagn. Res.*, vol. 117, pp. 321–337, Jan. 2011.
- [17] M. Ur-Rehman, Q. H. Abbasi, M. Akram, and C. Parini, "Design of band-notched ultra wideband antenna for indoor and wearable wireless communications," *IET Microwaves, Antennas Propag.*, vol. 9, no. 3, pp. 243–251, 2015.
- [18] H. K. Yoon, Y. J. Yoon, H. Kim, and C. Lee, "Flexible ultra-wideband polarisation diversity antenna with band-notch function," *IET Microwaves, Antennas Propag.*, vol. 5, no. 12, pp. 1463–1470, 2011.
- [19] V. Subba, "Design and implementation of dual notch band characteristics in UWB antenna for wireless personal communications," *Int. J. Adv. Trends Comput. Sci. Eng.*, vol. 6, pp. 1719–1725, Aug. 2019.
- [20] R. Mathur and S. Dwari, "Compact planar reconfigurable UWB-MIMO antenna with on-demand worldwide interoperability for microwave access/wireless local area network rejection," *IET Microwaves, Antennas Propag.*, vol. 13, no. 10, pp. 1684–1689, 2019.
- [21] S. Kingsly, D. Thangarasu, M. Kanagasabai, *et al.*, "Tunable band-notched high selective UWB filtering monopole antenna," *IEEE Trans. Antennas Propag.*, vol. 67, no. 8, pp. 5658–5661, 2019.
- [22] A. S. Eltrass and N. A. Elborae, "New design of UWB-MIMO antenna with enhanced isolation and dual-band rejection for WiMAX and WLAN systems," *IET Microwaves, Antennas*

Propag., vol. 13, no. 5, pp. 683–691, 2019.

- [23] M. Ghahremani, C. Ghobadi, J. Nourinia, M. S. Ellis, F. Alizadeh, and B. Mohammadi, “Miniaturised UWB antenna with dual-band rejection of WLAN/WiMAX using slitted EBG structure,” *IET Microwaves, Antennas Propag.*, vol. 13, no. 3, pp. 360–366, 2019.
- [24] C. Rong, W. Xiao, Y. Xu, and M. Y. Xia, “A double band-notched UWB antenna for flexible RF electronics,” *Appl. Comput. Electromagn. Soc. J.*, vol. 32, pp. 413–417, May 2017.
- [25] H. M. A. Rahman and M. Khan, “Design and analysis of a compact band notch UWB antenna for body area network,” *Journal of Electromagnetic Analysis and Applications*, vol. 10, pp. 157–169, Jan. 2018.
- [26] A. Majeed and K. Sayidmarie, “UWB elliptical patch monopole antenna with dual-band notched characteristics,” *Int. J. Electr. Comput. Eng.*, vol. 9, pp. 3591–3598, Oct. 2019.
- [27] Malaysian Communications and Multimedia Commission, *Guideline on the Provision of Wireless Local Area Network (WLAN) Service*, pp. 1–15, 2013.
- [28] Y. Gaurav and R. Chauhan, “A compact UWB BPF with a notch band using rectangular resonator sandwiched between interdigital structure,” *Int. J. Electr. Comput. Eng.*, vol. 7, pp. 2420, Oct. 2017.
- [29] X. Guan, Z. Wang, W. Huang, *et al.*, “Novel ultra-wideband antenna with quadruple band rejection characteristic for wearable applications,” in *Proc. IEEE International Workshop on Electromagnetics: Applications and Student Innovation Competition*, 2016.
- [30] M. Dwairi, “A planar UWB semicircular-shaped monopole antenna with quadruple band notch for WiMAX, ARN, WLAN, and X-band,” *Int. J. Electr. Comput. Eng.*, vol. 10, pp. 908–918, Feb. 2020.

Copyright © 2022 by the authors. This is an open access article distributed under the Creative Commons Attribution License ([CC BY-NC-ND 4.0](https://creativecommons.org/licenses/by-nc-nd/4.0/)), which permits use, distribution and reproduction in any medium, provided that the article is properly cited, the use is non-commercial and no modifications or adaptations are made.



Munirah Az Zahra Abdul Rashid received her bachelor degree in electrical engineering from Universiti Tun Hussein Onn Malaysia (UTHM), Parit Raja, Batu Pahat, Johor, Malaysia in 2018. She is currently working towards the M.S. degree in electrical engineering at UTHM. Her main research interests include microwave antennas, ultra-wideband (UWB) antennas and design of wearable UWB antennas with notch bands characteristics.



Shaharil Mohd Shah obtained his B.Eng. degree in microwave and communication from Multimedia University (MMU) in 2002. He received his M.Sc. degree in microwave engineering and wireless subsystems design from the University of Surrey, UK in 2004 and pursuing his Ph.D. degree in communication engineering from the University of Birmingham, UK before graduating in 2016. He is currently a senior lecturer in the

Department of Electronic Engineering, Faculty of Electrical and Electronic Engineering, Universiti Tun Hussein Onn Malaysia (UTHM). His research interests include, but not limited to, design of microwave devices, active and passive antennas and nonlinear characterisation of active devices.



Huda A Majid received the B.Eng. degree in electrical engineering (telecommunication) from Universiti Teknologi Malaysia, in 2007. He then obtained his M.Eng. degree in 2010 and Ph.D. degree in electrical engineering in 2013, at Universiti Teknologi Malaysia. He is currently a lecturer in the Department of Electrical Engineering Technology, Faculty of Engineering Technology, Universiti Tun Hussein Onn Malaysia. His research interest includes the areas of design of microstrip antennas, small antennas, Reconfigurable antennas, metamaterials structure, metalateral antennas and millimeter wave antennas. He has published over 90 articles in journals and conference papers.



Asmarashid Ponniran received the bachelor degree of electrical engineering from Universiti Tun Hussein Onn Malaysia (UTHM), Malaysia, in 2002 and master degree of engineering (electrical) from Universiti Teknologi Malaysia, Malaysia, in 2005. Then, he received the Ph.D. degree in energy and environment science from Nagaoka University of Technology, Japan, in 2016. He is currently an associate professor at UTHM. His research interests in power electronics area include power converter's circuit structure optimization, switching strategies for modular multilevel power converters, high power density achievement of power converters, high-voltage-gain power converters and high-frequency power converters. These research interests are toward renewable energy (RE), electric vehicle (EV), smart grid power system (SGPS) and data centre of power system (DCPS) applications.



Fazilah Hassan is a senior lecturer in Control and Mechatronics Department, School of Electrical Engineering, Universiti Teknologi Malaysia. She received her Ph.D. degree in engineering from the University of Lincoln, UK in 2018. She is currently a member of Advanced Control Research Group in UTM. Her research interests include robust control, fractional control, optimization and high speed tilting train.